
Comparison Between Prone and Upright Imaging of the Inferior Wall Using $^{201}\text{TlCl}$ Myocardial Perfusion SPECT

Koji Nakaya¹⁻³, Masahisa Onoguchi¹, Yoshihiro Nishimura³, Keisuke Kiso³, Hideki Otsuka⁴, Yoshifumi Nouno³, Takayuki Shibutani¹, and Eisuke Yasuda²

¹Department of Quantum Medical Technology, Graduate School of Medical Sciences, Kanazawa University, Ishikawa, Japan;

²Department of Radiological Technology, Faculty of Health Science, Suzuka University of Medical Science, Mie, Japan; ³Department of Radiology and Nuclear Medicine, National Cerebral and Cardiovascular Center Hospital, Osaka, Japan; and ⁴Department of Medical Imaging/Nuclear Medicine, Tokushima University Graduate School, Tokushima, Japan

Because it suppresses attenuation artifacts from the diaphragm, prone SPECT is suitable for evaluating the cardiac inferior wall. A solid-state dedicated cardiac camera allows upright imaging, which can also be used to avoid attenuation artifacts from the diaphragm. We compared prone and upright imaging for inferior wall evaluation using $^{201}\text{TlCl}$ myocardial perfusion SPECT (MPS). **Methods:** The study targeted 45 patients. The prone imaging group included 23 subjects who underwent additional prone imaging because supine imaging indicated that the inferior wall had reduced uptake. The upright imaging group included 22 subjects who, in the past, had shown reduced uptake in the inferior wall during supine imaging. Using the MPS stress images and analysis software, we created a polar map showing the incorporation of the radioisotope throughout the whole of the myocardium; this polar map was then classified into 17 segments. The percentage uptake ratios of the inferior/anterior wall were calculated for the prone and upright acquisitions. These ratios were used as the ratio of percentage uptake in each segment of the anterior wall to percentage uptake in each segment of the inferior wall. In addition, 6 reviewers visually evaluated the uniformity within the inferior wall for both the prone and the upright imaging. **Results:** There was a significant difference in percentage uptake ratios between the prone and upright images in segments 4/1 (basal inferior/basal anterior; $P < 0.05$), 11/12 (mid inferolateral/mid anterolateral; $P < 0.001$), and 15/13 (apical inferior/apical anterior; $P < 0.05$). There were no significant differences between the prone and upright images in visual evaluations of uniformity within the inferior wall. **Conclusion:** In comparison with upright imaging, prone imaging has a higher rate of suppression of attenuation artifacts from the diaphragm. However, this difference does not seem to affect the images visually. Therefore, upright and prone imaging can be used interchangeably to evaluate the inferior wall.

Key Words: inferior wall; prone imaging; upright imaging; myocardial perfusion SPECT

Received Jun. 20, 2017; revision accepted Sep. 11, 2017.

For correspondence or reprints contact: Masahisa Onoguchi, Department of Quantum Medical Technology, Graduate School of Medical Science, Kanazawa University, Kodatsuno 5-11-80, Kanazawa, Ishikawa 920-0942, Japan.

E-mail: onoguchi@staff.kanazawa-u.ac.jp

Published online Oct. 17, 2017.

COPYRIGHT © 2017 by the Society of Nuclear Medicine and Molecular Imaging.

J Nucl Med Technol 2017; 45:304–308

DOI: 10.2967/jnmt.117.197632

The solid-state dedicated cardiac camera (D-SPECT; Spectrum Dynamics) was recently introduced in Japan, and its use is increasing in facilities that treat patients who require myocardial perfusion SPECT (MPS) evaluation. This camera has increased sensitivity and resolution, and imaging can be performed at high speed (1–3). The D-SPECT can be used for upright imaging. Imaging with the conventional Anger-type device is performed with the patient supine, which limits evaluation of the inferior wall in some patients because of attenuation artifacts from the diaphragm. In such a case, we add prone imaging specialized for imaging the inferior wall. We can then evaluate myocardial perfusion using both images (4–7). Upright imaging with D-SPECT, however, can also depict the inferior wall, while attenuating the artifacts from the diaphragm (8). Hence, both imaging modalities can diagnose the inferior wall, but it is unknown which is superior. If upright imaging is inferior to prone imaging, it would be desirable to evaluate the inferior wall by adding prone imaging to the diagnostic protocol. In this study, we evaluated inferior wall uniformity using prone MPS imaging with a conventional camera and upright MPS imaging with $^{201}\text{TlCl}$ and the D-SPECT camera.

MATERIALS AND METHODS

Patients

From March 1, 2013, to July 30, 2014, we retrospectively enrolled 23 patients who had undergone prone imaging with a conventional camera (the prone group). The additional prone imaging was performed in these patients because evaluation of the inferior wall was limited in the supine imaging. None of the patients in this prone group had coronary artery disease. Patients without coronary artery disease had a stenosis rate of less than 50% during coronary angiography. Among patients who had not undergone coronary angiography, we chose those whose left ventricular ejection fraction was more than 55% during echocardiography. In addition, from March 1, 2015, to August 31, 2015, 22 patients who underwent

upright imaging with D-SPECT were enrolled (the upright group). These patients had previously undergone supine imaging, which had allowed limited evaluation of the inferior wall. The method for selecting healthy patients from this group was the same as that for selecting healthy patients from the prone group.

The ethics committee at the National Cerebral and Cardiovascular Center in Japan approved this retrospective study, and the requirement to obtain informed consent was waived.

MPS Acquisition and Processing

We used stress ^{201}Tl MPS images. First, 111 MBq of ^{201}Tl were administered intravenously. Patient data with ergometer stress were used, and we obtained stress SPECT images in the supine and prone positions using the conventional camera and upright images using the D-SPECT protocol.

For the prone images collected by the conventional camera, we used 2 BrightView detector-type γ -cameras (Philips). To collect the data, we used a cardiac high-resolution collimator designed for the heart, with 2 detectors positioned at 90° angles. We collected the data with prone imaging at 6° intervals over 180° (15 s/step, 3.75 min in total) using a step-and-shoot mode. The filtering conditions for the SPECT image reconstruction included a matrix of 64×64 , amplification of 1.85 times, and a pixel size of 2.72 mm. Maximum-likelihood expectation maximization was used for image reconfiguration. A Butterworth filter (order, 10; cutoff frequency, 0.50 cycle/cm) was used as the preprocessing filter, and Cardio Bull analysis software (Fujifilm RI Pharma Co.) was used for image processing. We did not perform attenuation or scatter correction.

To collect data for upright imaging by D-SPECT, we used a wide-angle tungsten collimator. The material of the semiconductor detector was cadmium-zinc-telluride. The collection time ended when left ventricular counts reached 1.5 million. The conditions for filtering during SPECT image reconstruction included a field of view of 160 mm, amplification of 1 time, and a pixel size of 2.26 mm. Ordered-subset expectation maximization was used for image reconfiguration, the reconstruction condition was 7 iterations and 32 subsets, and Cardio Bull software was used for image processing. We did not correct for attenuation or scatter.

Percentage Uptake Ratio in Inferior/Anterior Wall

We created a polar map using the MPS stress images and classified it into 17 segments (Fig. 1). Using this 17-segment classification, the percentage uptake ratios of the inferior/anterior wall were calculated for the prone and upright images of both groups. The percentage uptake ratios were the ratio of percentage uptake in each segment of the anterior wall to percentage uptake in each segment of the inferior wall. This ratio was calculated for segments 3/2 (basal inferoseptal/basal anteroseptal), 4/1 (basal inferior/basal

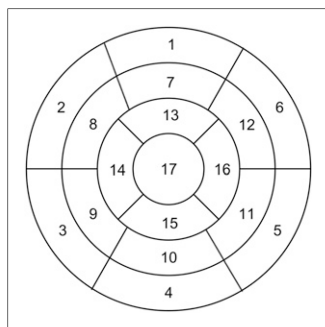


FIGURE 1. 17-segment classification of polar map.

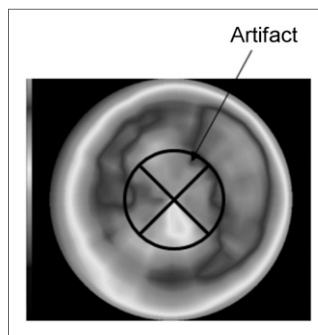


FIGURE 2. Apical artifact appearing with upright D-SPECT imaging.

anterior), 5/6 (basal inferolateral/basal anterolateral), 9/8 (mid inferoseptal/mid anteroseptal), 10/7 (mid inferior/mid anterior), 11/12 (mid inferolateral/mid anterolateral), and 15/13 (apical inferior/apical anterior), except for the apex, because SPECT images from upright imaging with D-SPECT may show a large decrease in artifacts in the apex. An example of this artifact is shown in Figure 2. The percentage uptake ratios for the prone and upright images in both groups were compared.

Visual Uniformity of Inferior Wall

Six reviewers independently evaluated the uniformity of the inferior wall on prone or upright MPS images from both groups. MPS images used 3 axes (short, horizontal, and vertical). This evaluation examined only uniformity within the inferior wall, scoring it as 1 (poor), 2 (fair), 3 (average), 4 (good), or 5 (excellent) for each imaging position. The mean of each reviewer's scores was calculated, and the average scores of the two groups were compared.

Statistical Analysis

The Mann-Whitney U test was used to evaluate differences in percentage uptake ratios and in average visual scores between prone and upright imaging.

RESULTS

Physical Evaluation

The patient information for the prone and upright groups is shown in Table 1. Age, height, body weight, and body mass index were 69 ± 10 , 1.67 ± 0.05 , 64.5 ± 6.02 , and 23.2 ± 1.79 , respectively, in the prone group and 74 ± 4 , 1.66 ± 0.06 , 64.5 ± 9.40 , and 23.3 ± 2.42 , respectively, in the upright group. Age, sex, height, body weight, and body mass index did not significantly differ between the prone and upright groups, nor did the coronary risk factors, blood sampling data, or study protocol.

The percentage uptake ratios for the prone and upright images are shown in Figure 3. The ratios for the upright image in segments 3/2, 4/1, 5/6, 9/8, 10/7, 11/12, and 15/13 were 0.90 ± 0.12 , 0.84 ± 0.09 , 0.92 ± 0.06 , 0.95 ± 0.04 , 0.88 ± 0.06 , 0.90 ± 0.04 , and 0.89 ± 0.07 , respectively. The ratios significantly differed between the prone and upright images in segments 4/1 ($P < 0.05$), 11/12 ($P < 0.001$), and 15/13 ($P < 0.05$) and did not significantly differ in segments 3/2, 5/6, 9/8, and 10/7.

Visual Evaluation

The 6 reviewers gave evaluation scores above 3 for all patients. The mean \pm SD of the average scores in the prone

TABLE 1
Clinical Characteristics of Patients in Prone and Upright Imaging Groups

Characteristic	Prone group (n = 23)	Upright group (n = 22)
Age (y)	69 ± 10	74 ± 4
Male (n)	23 (100%)	22 (100%)
Height (m)	1.67 ± 0.05	1.66 ± 0.06
Body weight (kg)	64.5 ± 6.02	64.5 ± 9.19
Body mass index	23.2 ± 1.79	23.3 ± 2.37
Coronary risk factors		
Smoking	14 (60.8%)	18 (78.2%)
Hypertension	18 (78.3%)	18 (78.2%)
Hyperlipidemia	16 (69.6%)	18 (78.2%)
Diabetes mellitus	10 (43.5%)	7 (30.4%)
Familial hypercholesterolemia	4 (17.4%)	8 (34.7%)
Impaired glucose tolerance	0 (0%)	1 (4.3%)
Other factors		
Blood glucose	128.7 ± 63.2	120.3 ± 36.2
Hemoglobin A1c	6.30 ± 0.87	6.57 ± 0.72
High-density-lipoprotein cholesterol	54.6 ± 11.6	49.9 ± 14.4
Low-density-lipoprotein cholesterol	90.9 ± 24.4	87.9 ± 19.4
Study protocol		
Exercise time	8 min 9 s	7 min 26 s
Maximum stress (watt [%])	121.7 ± 24.8	110.2 ± 24.6
(Target heart rate/maximum heart rate) × 100 (%)	91.7 ± 11.4	87.9 ± 19.4
Patients reaching target heart rate (n)	8 (34.7%)	7 (30.4%)
Maximum blood pressure (mm Hg)	205.8 ± 25.8	196.7 ± 28.5
Patients in whom ST changed on electrocardiography (n)	3 (13.0%)	2 (8.70%)

There were no significant differences between the prone and upright groups.

and upright groups were 3.9 ± 0.3 and 3.9 ± 0.3 , respectively. The visual evaluations of uniformity within the inferior wall did not significantly differ between the prone and upright groups.

DISCUSSION

We compared inferior wall uniformity between prone and upright imaging. Patients without coronary artery disease were chosen from both the prone and the upright

groups on the basis of the coronary angiography or echocardiography results. Because patients without coronary artery disease might not have undergone coronary angiography, they underwent echocardiography. The prone and upright groups did not significantly differ in age, sex, height, body weight, body mass index, coronary risk factors (smoking habit, hypertension, hyperlipidemia, diabetes mellitus, family history, and impaired glucose tolerance), other factors (blood glucose, hemoglobin A1c, high-density-lipoprotein cholesterol, and

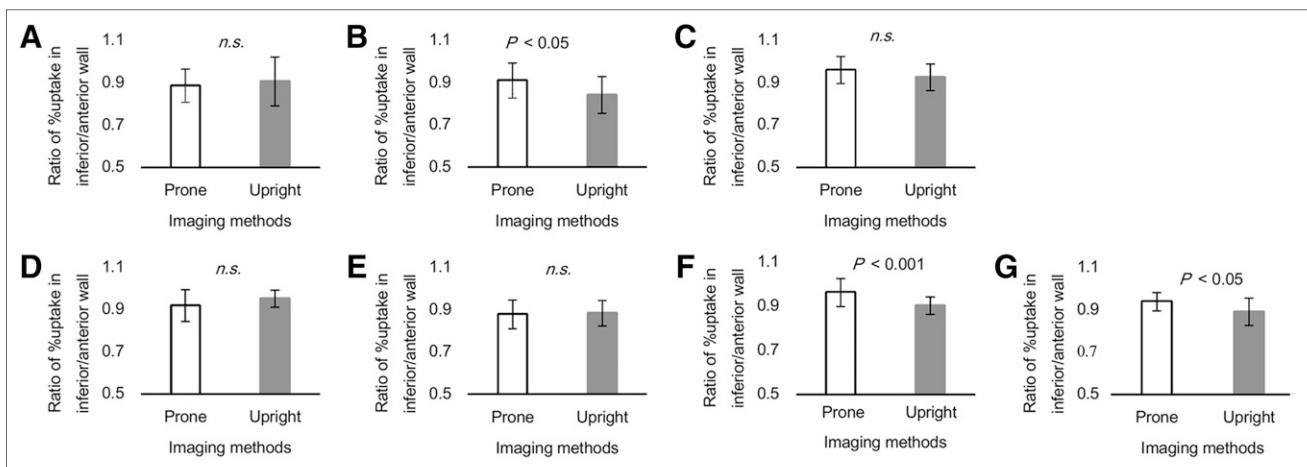


FIGURE 3. Percentage uptake ratios for prone and upright images. Mann–Whitney *U* test was used to show significant differences between imaging methods. (A) Segment 3/2. (B) Segment 4/1. (C) Segment 5/6. (D) Segment 9/8. (E) Segment 10/7. (F) Segment 11/12. (G) Segment 15/13.

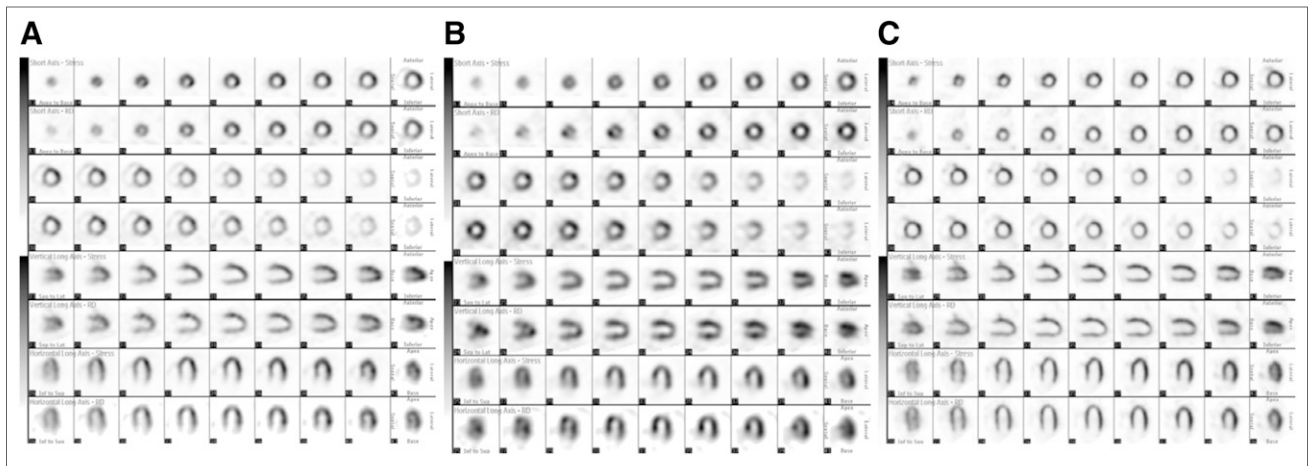


FIGURE 4. Supine (A), prone (B), and upright (C) SPECT images in same patient. Top row of each set is stress image, and bottom row is resting image.

low-density-lipoprotein cholesterol), or study protocol (exercise time, maximum stress [watt (%)], number of people reaching target heart rate, maximum blood pressure, and electrocardiography findings).

The prone group included 23 patients and the upright group 22 patients. Currently, our hospital does not perform prone imaging with a conventional camera. When the D-SPECT camera was introduced, the hospital began using upright imaging on this camera for all MPS examinations. Therefore, we could not improve the statistical strength of the study by increasing the number of patients without coronary artery disease who underwent prone imaging; only the 23 patients were available. In addition, for our evaluation of the inferior wall, we included only male patients even though female patients with large breasts may also show artifacts in the inferior wall. In a future study, we would like to extend this evaluation to women with large breasts.

We used a ^{201}Tl formulation. MPS requires a larger radiation exposure dose with ^{201}Tl than with $^{99\text{m}}\text{Tc}$ -tetrofosmin. Hence, there are many clinical and academic reports of $^{99\text{m}}\text{Tc}$ -tetrofosmin imaging. ^{201}Tl , however, has the advantage of being administered as a single dose for both stress and resting imaging. Many facilities in Japan thus use ^{201}Tl to reduce the personnel needed. We used ^{201}Tl for this study because it is what our hospital primarily uses.

On physical evaluation, we calculated the percentage uptake ratios of the inferior/anterior wall in each segment. We compared the ratios for the prone group with those for the upright group. The upright ratios were significantly lower than the prone ratios in segments 4/1, 11/12, and 15/13. An artifact peculiar to upright imaging may appear in the apex of the heart (8,9); segments 11 and 15, which correspond to the inferior wall, are right coronary artery territories, but in the upright group this artifact caused the percentage uptake in these segments to decrease. Therefore, the rate of inhibition of diaphragmatic attenuation artifacts in segment 4 was lower in upright imaging than in prone

imaging. As far as image quality is concerned, prone imaging is known to suppress attenuation artifacts from the diaphragm better than upright imaging. This physical evaluation gave the same result.

Six reviewers visually compared uniformity within the inferior wall between the prone and upright images and found no significant differences. However, although visual uniformity is affected by attenuation artifacts, it is also affected by the type of device being used, and visual uniformity and attenuation artifacts are largely different issues. The high resolution of the D-SPECT semiconductor detector improves uniformity. One must understand that upright imaging not only suppresses diaphragmatic artifacts but also increases resolution.

Both sets of MPS images from a single patient are shown in Figure 4. In this patient, supine imaging suffered from a diaphragmatic attenuation artifact. This artifact was reduced on prone and upright imaging, with prone imaging seeming to better suppress the artifact than upright imaging. However, visual evaluations of the inferior wall were equal for both acquisitions. Therefore, the utility of evaluating the inferior wall by adding prone imaging with a conventional camera was demonstrated, and upright D-SPECT imaging allowed evaluation of the inferior wall without the additional requirement of prone imaging.

With a conventional SPECT camera, the detector rotates around the patient, resulting in an artifact induced by the presence of the lowered hands. In contrast, with the D-SPECT camera, the position of the detector is fixed around the chest, allowing the images to be collected without rotating the detector (2). Upright imaging allows both hands to be placed on the detector while the images are collected. Thus, upright imaging is easier on the patient because body posture is stable, and the patient is relaxed because the parasympathetic nervous system is activated. Because the patient does not have to raise both hands during image collection, there is no body movement to affect visualization of the inferior wall.

In addition, upright imaging is advantageous from the viewpoint of respiration. Prone imaging affects respiration

because of the difference in diaphragmatic movement between chest breathing and abdominal breathing. Movement of the diaphragm tends to be greater in abdominal breathing than in chest breathing (10). The prone position places pressure on the abdomen, causing chest breathing to become dominant. Consequently, we believe that prone imaging suppresses movement of the diaphragm and is thus preferable for depicting the inferior wall. In contrast, upright imaging does not demand the up-thrust of the abdominal organs against gravity, making breathing easier because the breathing area is expanded. Being performed with the patient in a relaxed state, upright imaging is thought to suppress movement of the diaphragm. Thus, both imaging methods enable evaluation of the inferior wall with respect to breathing-related artifacts.

This study was limited in that it compared data collected on different devices. A difference occurs under every condition because the devices were different. Comparison of upright and prone imaging on the same device would of course be desirable, but in our study, the prone imaging was performed on a conventional camera instead of a D-SPECT camera. As for image processing, the Butterworth filter parameters during the SPECT acquisition were set to differ between the two devices so that the quality of the images would be similar. In addition, in both cases, image analysis was performed by the same software program (Cardio Bull) and in the same way.

Another limitation is that we did not evaluate the inferior wall in patients with a right coronary artery stenosis. Ideally, such an evaluation should be performed on the same study population, but our limited number of cases made this impossible.

In the present study, we compared inferior wall uniformity from both physical and visual evaluations in patients without coronary artery disease, and we found that the uniformity was similar. We believe the purpose of this study was achieved because our findings suggest that an inferior wall irregularity can be diagnosed using upright imaging without the addition of prone imaging.

CONCLUSION

Prone imaging better suppresses diaphragmatic attenuation artifacts than upright imaging; however, this difference

does not seem to affect the images visually. Therefore, upright imaging with D-SPECT allows evaluation of the inferior wall without requiring additional prone imaging.

DISCLOSURE

No potential conflict of interest relevant to this article was reported.

ACKNOWLEDGMENTS

We thank the staff of the National Cerebral and Cardiovascular Center for their help with preparing the manuscript. We also deeply appreciate the support we received from Keizo Takatoku and Masashi Kawakane from FUJIFILM RI Pharma Co., and Yasuhiro Imanishi and Atsushi Miyata from Suzuka General Hospital.

REFERENCES

1. Sharir T, Ben-Haim S, Merzon K, et al. High-speed myocardial perfusion imaging: initial clinical comparison with conventional dual detector Anger camera imaging. *JACC Cardiovasc Imaging*. 2008;1:156–163.
2. Erlandsson K, Kacperski K, van Gramberg D, Hutton BF. Performance evaluation of D-SPECT: a novel SPECT system for nuclear cardiology. *Phys Med Biol*. 2009;54:2635–2649.
3. Nakazato R, Tamarappoo BK, Kang X, et al. Quantitative upright-supine high-speed SPECT myocardial perfusion imaging for detection of coronary artery disease: correlation with invasive coronary angiography. *J Nucl Med*. 2010;51:1724–1731.
4. Esquerré JP, Coca FJ, Martínez SJ, Guiraud RF. Prone decubitus: a solution to inferior wall attenuation in thallium-201 myocardial tomography. *J Nucl Med*. 1989;30:398–401.
5. Segall GM, Davis MJ, Golis ML. Improved specificity of prone versus supine thallium SPECT imaging. *Clin Nucl Med*. 1988;13:915–916.
6. Segall GM, Davis MJ. Prone versus supine thallium myocardial SPECT: a method to decrease artifactual inferior wall defects. *J Nucl Med*. 1989;30:548–555.
7. Katayama T, Ogata N, Tsuruya Y. Diagnostic accuracy of supine and prone thallium-201 stress myocardial perfusion single-photon emission computed tomography to detect coronary artery disease in inferior wall of left ventricle. *Ann Nucl Med*. 2008;22:317–321.
8. Hain SF, Van Gramberg D, Bomanji JB, Kayani I, Groves AM, Ben-Haim S. Can upright myocardial perfusion imaging be used alone with a solid-state dedicated cardiac camera? *Q J Nucl Med Mol Imaging*. 2013;57:383–390.
9. Allie R, Hutton BF, Prvulovich E, Bomanji J, Michopoulou S, Ben-Haim S. Pitfalls and artifacts using the D-SPECT dedicated cardiac camera. *J Nucl Cardiol*. 2016;23:301–310.
10. Hussain SN, Rabinovitch B, Macklem PT, Pardy RL. Effect of separate rib cage and abdominal restriction on exercise performance in normal humans. *J Appl Physiol*. 1985;58:2020–2026.